LA-UR-21-22043
Approved for public release; distribution is unlimited.

Title: Impact of nuclear data validation with uncertainty quantification and diverse benchmarks on criticality safety

Author(s): Clark, Alexander Rich

Intended for: Interview for Scientist 2 position in XCP-7: Radiation Transport Applications

Issued: 2021-03-01

Impact of nuclear data validation with uncertainty quantification and diverse benchmarks on criticality safety

Alexander R. Clark, Ph.D., E.I.

XCP-5: Materials and Physical Data

March 3rd, 2021

Interview for Scientist 2 position in XCP-7: Radiation Transport Applications

LA-UR-21-xxxxx

Outline

Dissertation research

- Introduction and motivation
- Model calibration process
- Model calibration applied to neutron multiplicity counting (NMC) measurements
- Summary and conclusions

Postdoctoral research

- Introduction and motivation
- Pulsed-sphere measurements
- SA applied to pulsed-sphere TOF spectra
- Summary and future work

Benefits to criticality safety

- Nuclear data adjustment accounting for random and systematic uncertainties resulted in improved neutron multiplicity counting simulations
- Combination of critical benchmarks and pulsed sphere measurements in nuclear data validation can provide tighter constraint on fission parameters

Using neutron multiplicity counting to adjust cross sections

- Cross section evaluation via critical experiments and reaction rate measurements has led to their over-calibration for some applications
- ENDF/B-VII.1 cross sections (Pu-239 $\bar{\nu}$) do not adequately predict subcritical experiments
- Neutron multiplicity counting (NMC) is a method of non-destructive analysis of SNM assemblies
  - Each NMC distribution moment is a function of the cross sections raised to the power of the moment's order
  - Higher-order NMC distribution moments are more sensitive to the cross sections than the mean (first moment)
  - Model calibration applied to higher-order NMC distribution moments produced more accurately simulated NMC experiments with reduced uncertainty

Characteristics of neutron multiplicity counting

- Neutron multiplicity counting (NMC) accumulates distribution of coincident neutron counts
- Independent neutron emissions characterized by Poisson distribution
- Fission-chain reactions are described by generalized Poisson distribution
- Excess variance in NMC distribution is characteristic of multiplying material
- Need higher-order NMC distribution moments to characterize SNM assemblies

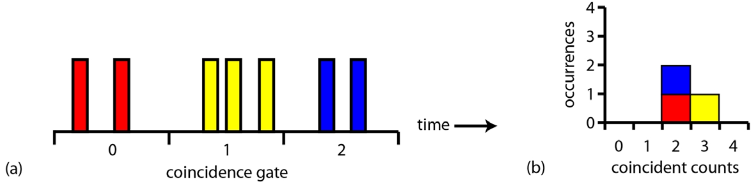

Accumulation of NMC distribution

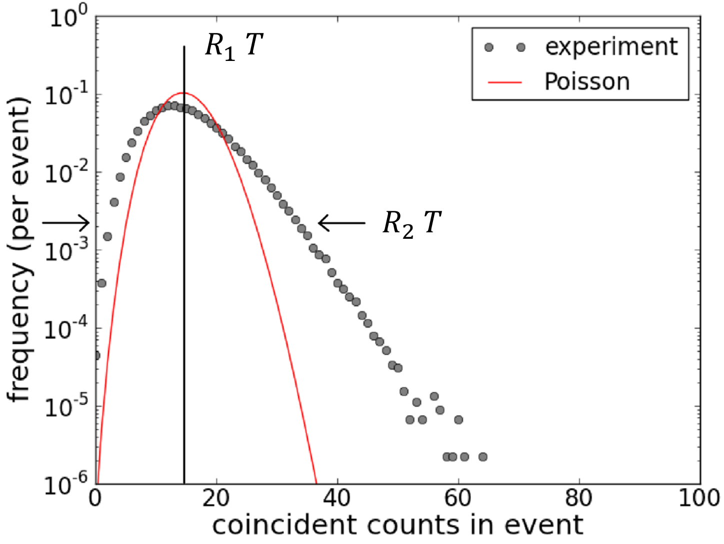

NMC and Poisson distributions with the same mean

Adjusting the Pu-239 $\bar{\nu}$ to better predict counting distribution

- Simulations of NMC of a 4.5-kg sphere of weapons-grade plutonium metal (BeRP ball) overpredicted NMC distribution moments
- Small reduction in Pu-239 $\bar{\nu}$ improved accuracy of simulated moments
- ENDF/B-VII.1 Pu-239 $\bar{\nu}$ adjusted to match JEZEBEL critical experiments

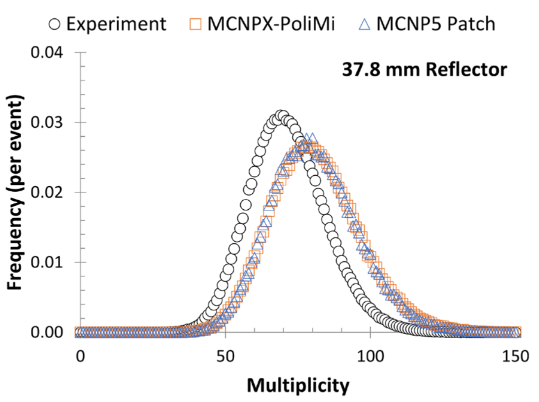

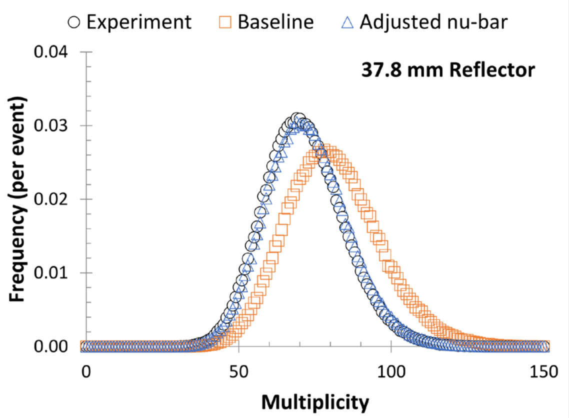

Simulated NMC distribution before (top) and after (bottom) Pu-239 $\bar{\nu}$ adjustment

Model calibration overview

Sensitivity Analysis (SA)

- Adjoint-based first derivatives
- Sensitivity of detector response to cross sections

Uncertainty Quantification (UQ)

- First-order propagation of uncertainty
- Detector response covariance

Parameter Estimation (PE)

- Model calibration
- Best-estimate cross sections and covariances

Sensitivity Analysis (SA)

- Adjoint-based first derivatives
- Sensitivity of detector response to cross sections

Uncertainty Quantification (UQ)

- First-order propagation of uncertainty
- Detector response covariance

Parameter Estimation (PE)

- Model calibration
- Best-estimate cross sections and covariances

Description of the forward transport equation

- Describes a balance of production and loss terms for expected number of neutrons:

$$L\psi = \overbrace{Q}^{\text{intrinsic source}} = \bar{\nu}_{sf} S$$

$$L = \underbrace{\hat{\Omega}\cdot\nabla}_{\text{streaming loss}} + \overbrace{\Sigma_t}^{\substack{\text{total}\\\text{interaction loss}}} - \underbrace{\int_{4\pi} d\Omega' \int_0^\infty dE' \Sigma_s}_{\text{scatter source}} - \overbrace{\frac{\chi}{4\pi}\int_{4\pi} d\Omega' \int_0^\infty dE' \bar{\nu}\Sigma_f}^{\text{fission source}}$$

L: Forward transport operator
ψ: Forward angular flux
S: Spontaneous fission source rate density and spectrum

Σ_t, Σ_s,$\bar{\nu}\Sigma_f$: Macroscopic total, scatter, and fission neutron production cross sections
χ: Fission neutron energy spectrum

Description of the adjoint transport equation

- Counterpart to the forward NTE:

$$L^{*}\psi_1^{*} = Q_1^{*}$$

$$L^{*} = -\widehat{\Omega}\cdot\nabla + \Sigma_t - \int_{4\pi} d\Omega' \int_0^{\infty} dE'\Sigma_s - \bar{\nu}\Sigma_f \int_{4\pi} d\Omega' \int_0^{\infty} dE' \frac{\chi}{4\pi}$$

  - L^{*}: adjoint transport operator
  - ψ_1^{*}: Adjoint flux, “importance” of source neutrons to the mean count rate

Second-moment adjoint transport equation

$$L^* \psi_2^* = Q_2^*$$

$$Q_2^* = \overline{\nu(\nu - 1)} \Sigma_f I_1^2$$

$$I_1 = \int d\Omega' \int dE' \frac{\chi}{4\pi} \psi_1^*$$

- Obtained from Muñoz-Cobo stochastic transport equation
- L^* is the usual adjoint transport operator
- Q_2^* is defined in terms of ψ_1^*
- ψ_2^* is calculable using a standard transport solver

Form of the detector response moments

- First-moment detector response (mean count rate):

$$R_1 = \langle \psi, Q_1^* \rangle = \langle \psi, \sigma_d \rangle$$

- Equations for higher-order adjoint fluxes have the same form as usual adjoint NTE with special fixed-source terms:

$$L^* \psi_q^* = Q_q^*, q = 1,2, \dots$$

- Higher-order detector responses are computed like R_1:

$$R_q = \left\langle \psi, Q_q^* \right\rangle + \left\langle S, Q_{q,sf}^* \right\rangle$$

Second-moment detector response

$$R_2 = \langle \psi, Q_2^* \rangle + \left\langle S, Q_{2,sf}^* \right\rangle$$

$$Q_2^* = \overline{\nu(\nu-1)\Sigma_f} I_1^2,\; Q_{2,sf}^* = \overline{\nu(\nu-1)}_{sf} I_{1,sf}^2$$

$$I_1 = \int d\Omega' \int dE' \frac{\chi}{4\pi} \psi_1^*,\; I_{1,sf} = \int d\Omega' \int dE' \frac{\chi_{sf}}{4\pi} \psi_1^*$$

- ψ_1^* is a function of the cross sections to the first power
- Q_2^* is proportional to the square of the cross sections

Benefit of adjoint-based sensitivity analysis

- Adjoint-based approach allows the sensitivity to be computed with few transport solves

$$\frac{\partial R_1}{\partial \alpha} = \left\langle \frac{\partial Q_1^*}{\partial \alpha}, \psi \right\rangle + \left\langle \psi_1^*, \frac{\partial Q}{\partial \alpha} - \frac{\partial L}{\partial \alpha} \psi \right\rangle$$

- Derivative of flux is computationally expensive because it implicitly depends on the cross sections
- Sensitivity of higher-order detector response moments have a similar form

Sensitivity Analysis (SA)

- Adjoint-based first derivatives
- Sensitivity of detector response to cross sections

Uncertainty Quantification (UQ)

- First-order propagation of uncertainty
- Detector response covariance

Parameter Estimation (PE)

- Model calibration
- Best-estimate cross sections and covariances

Uncertainty quantification for measured responses

- Contribution from random source of uncertainty
  - Relative response uncertainty reduced by longer counting
- Contribution from systematic source of uncertainty
  - Cannot physically vary most measurement parameters
  - Instead quantify sensitivities via varying measurement parameters in high-fidelity simulations
  - Response uncertainty reduced by knowing the measurement parameters more precisely

$$[\mathrm{cov}(\boldsymbol{R}_m, \boldsymbol{R}_m)]_{\boldsymbol{p}} = \left(\frac{\partial \boldsymbol{R}_m}{\partial \boldsymbol{p}} \bigg|_{\boldsymbol{p}=\boldsymbol{p}^0} \right)^T \mathrm{cov}(\boldsymbol{p}, \boldsymbol{p}) \left(\frac{\partial \boldsymbol{R}_m}{\partial \boldsymbol{p}} \bigg|_{\boldsymbol{p}=\boldsymbol{p}^0} \right)$$

- Covariance between measured responses

$$\mathrm{cov}(\boldsymbol{R}_m, \boldsymbol{R}_m) = [\mathrm{var}(\boldsymbol{R}_m)]_N + [\mathrm{cov}(\boldsymbol{R}_m, \boldsymbol{R}_m)]_{\boldsymbol{p}}$$

Uncertainty quantification for simulated responses

- Contribution from model representation errors
  - Quantified via varying features of the experiment or the phase-space discretization
  - Response uncertainty reduced via higher-fidelity simulations
- Contribution from nuclear cross sections
  - Cross section covariances are determined from cross section measurement uncertainty
  - Response uncertainty reduced by knowing cross sections more precisely or through model calibration

$$[\mathrm{relcov}(\boldsymbol{R},\boldsymbol{R})]_{\alpha} = \boldsymbol{S}_{\boldsymbol{R},\boldsymbol{\alpha}}^{\mathrm{T}}\,\mathrm{relcov}(\boldsymbol{\alpha},\boldsymbol{\alpha})\boldsymbol{S}_{\boldsymbol{R},\boldsymbol{\alpha}}$$

- Covariance between simulated responses

$$\mathrm{relcov}(\boldsymbol{R},\boldsymbol{R}) = [\mathrm{relcov}(\boldsymbol{R},\boldsymbol{R})]_{\alpha}$$

Sensitivity Analysis (SA)

- Adjoint-based first derivatives
- Sensitivity of detector response to cross sections

Uncertainty Quantification (UQ)

- First-order propagation of uncertainty
- Detector response covariance

Parameter Estimation (PE)

- Model calibration
- Best-estimate cross sections and covariances

Model calibration using an extended Kalman filter

- Determine best-estimate cross sections and covariances that give optimum agreement between measured and simulated responses
- Bayesian inference method can use prior information about cross section distribution
- Nominal cross section values and corresponding covariances may be described by a multivariate Gaussian distribution
- Extended Kalman filter (EKF) is a method that produces best-estimate cross sections and covariances by using:
  - Prior cross section distribution
  - Measured NMC distribution moments

Extended Kalman filter algorithm

- Prediction step

$$R_q^0 = \langle \psi, Q_q^* \rangle|_{\alpha=\alpha^0} + \langle S, Q_{q,sf}^* \rangle|_{\alpha=\alpha^0}, \quad \mathrm{cov}(\boldsymbol{R}^0, \boldsymbol{R}^0) = \left(\frac{\partial \boldsymbol{R}^0}{\partial \boldsymbol{\alpha}} |_{\alpha=\alpha^0} \right)^{\boldsymbol{T}} \mathrm{cov}(\boldsymbol{\alpha}^0, \boldsymbol{\alpha}^0) \left(\frac{\partial \boldsymbol{R}^0}{\partial \boldsymbol{\alpha}} |_{\alpha=\alpha^0} \right)$$

- Update step

$$\boldsymbol{K} = \frac{\mathrm{cov}(\boldsymbol{\alpha}^0, \boldsymbol{\alpha}^0) \left(\frac{\partial \boldsymbol{R}^0}{\partial \boldsymbol{\alpha}} |_{\alpha=\alpha^0} \right)}{\mathrm{cov}(\boldsymbol{R}_m, \boldsymbol{R}_m) + \mathrm{cov}(\boldsymbol{R}^0, \boldsymbol{R}^0)}$$

$$\boldsymbol{\alpha}^1 = \boldsymbol{\alpha}^0 + \boldsymbol{K}(\boldsymbol{R}_m - \boldsymbol{R}^0), \quad \mathrm{cov}(\boldsymbol{\alpha}^1, \boldsymbol{\alpha}^1) = \left(\boldsymbol{I} - \boldsymbol{K} \left(\frac{\partial \boldsymbol{R}^0}{\partial \boldsymbol{\alpha}} |_{\alpha=\alpha^0} \right)^{\boldsymbol{T}} \right) \mathrm{cov}(\boldsymbol{\alpha}^0, \boldsymbol{\alpha}^0)$$

Detector response and sensitivity calculations

- Obtained 44-group cross sections and their covariances from SCALE
- Performed 1D PARTISN simulations of NMC of BeRP ball with nPod
  - Bare and 3.8 cm polyethylene-reflected configurations
  - Simplified composition of plutonium metal (Pu-239, 240) and polyethylene reflector (H-1, C-12)
  - nPod modeled as adjoint source on outer boundary

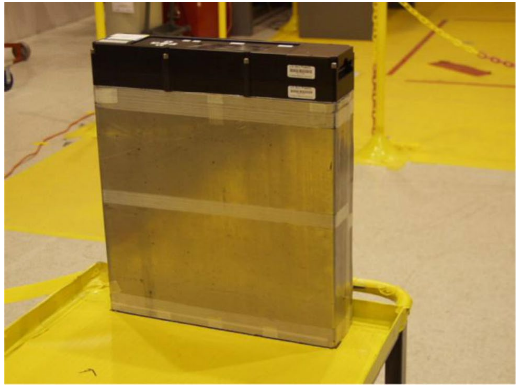

nPod neutron multiplicity counter

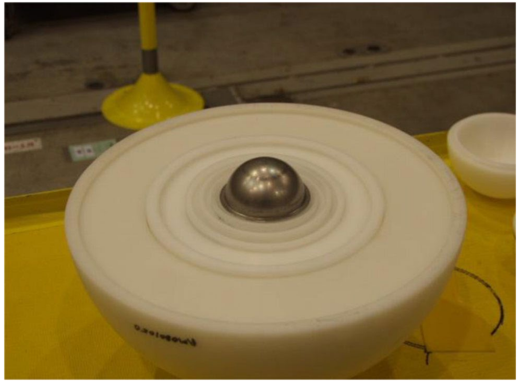

BeRP ball nested in polyethylene reflectors

R_1 and R_2 relative sensitivity totals

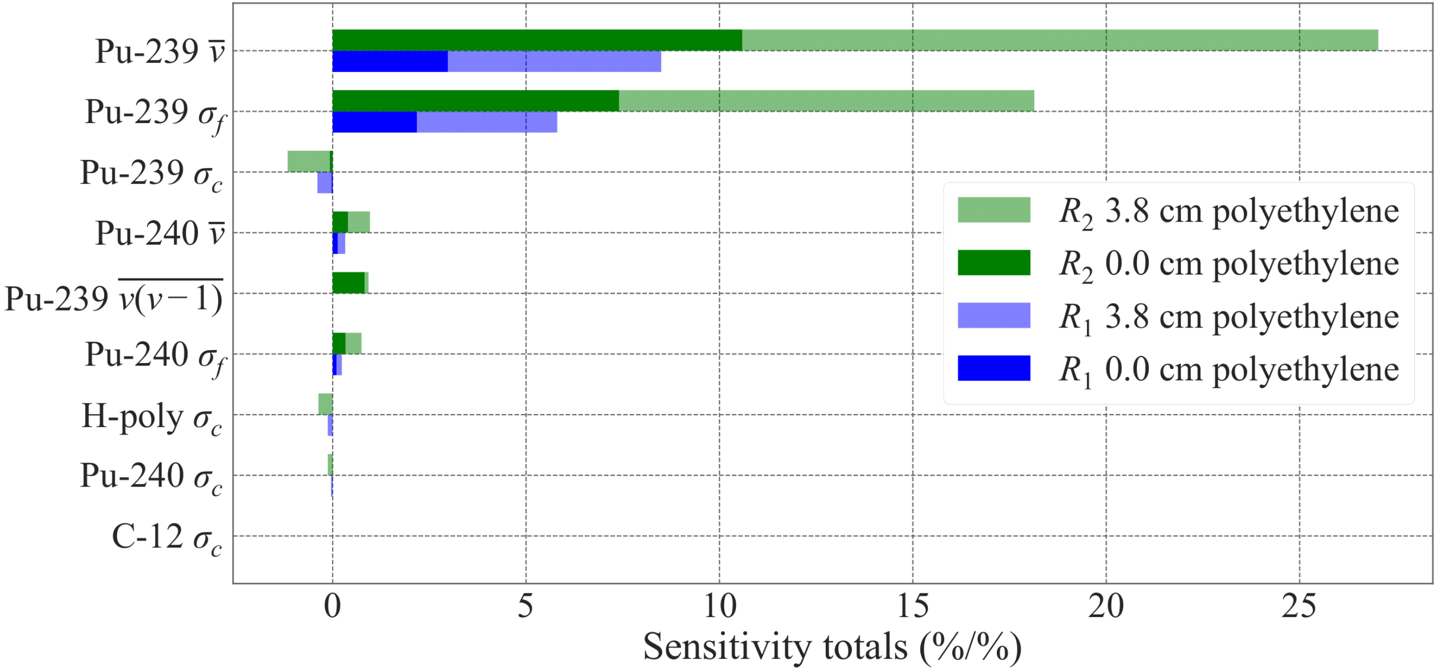

Sensitivity totals for the measured R_1 and R_2

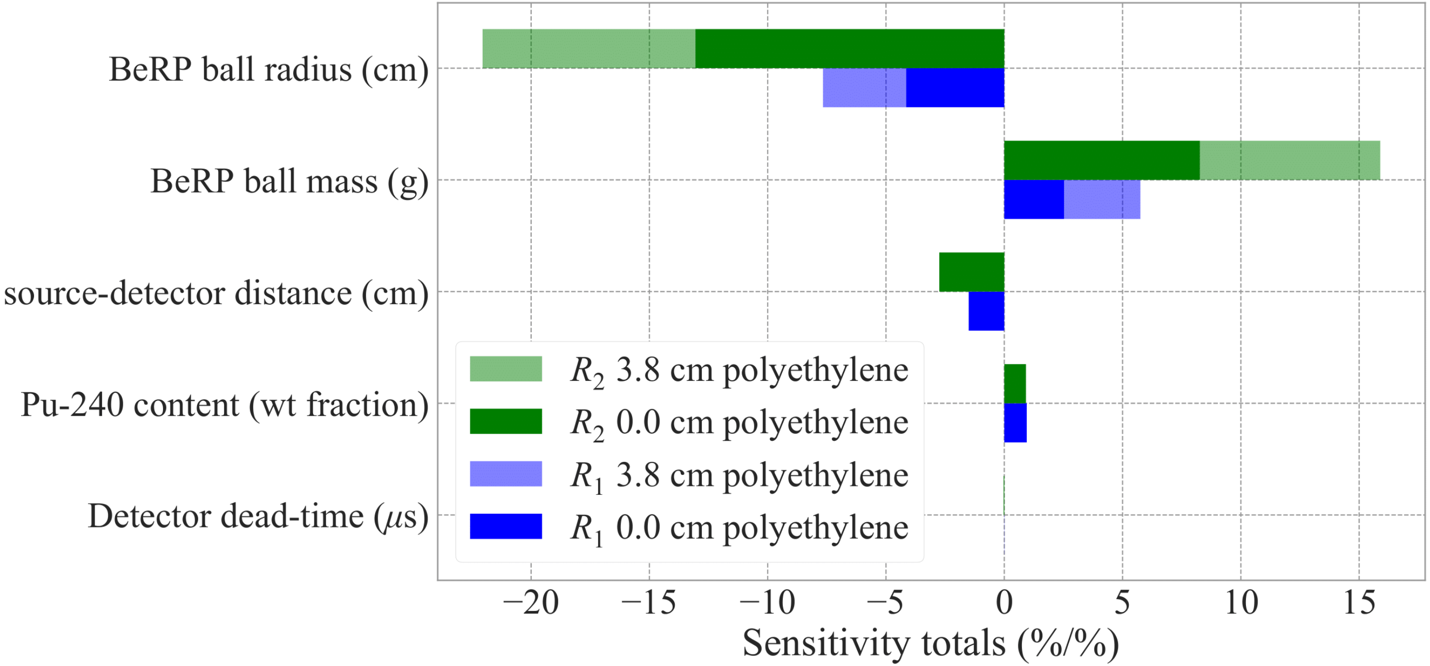

Nominal and adjusted cross section correlations

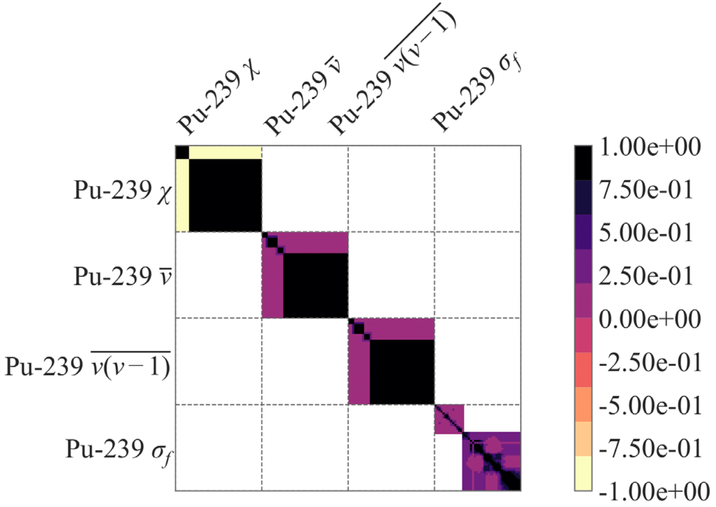

Correlations between the cross sections before the model calibration

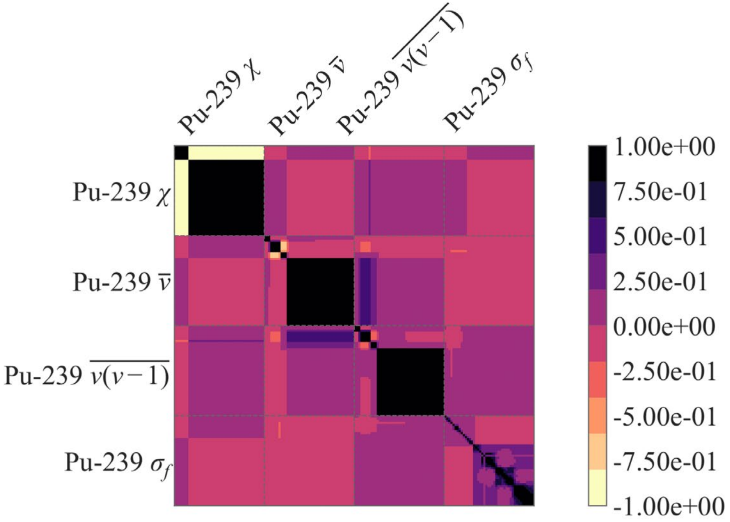

Correlations between the cross sections after the model calibration

Measured and simulated response correlations

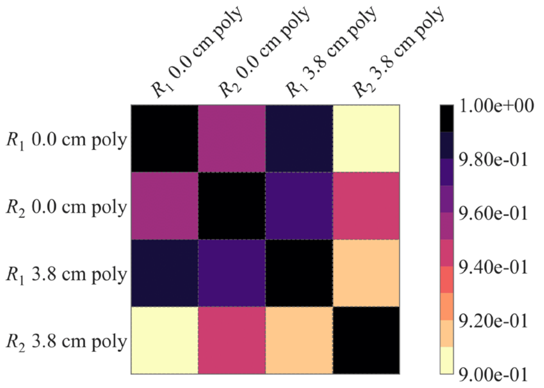

Correlations between the measured responses due to the measurement parameters

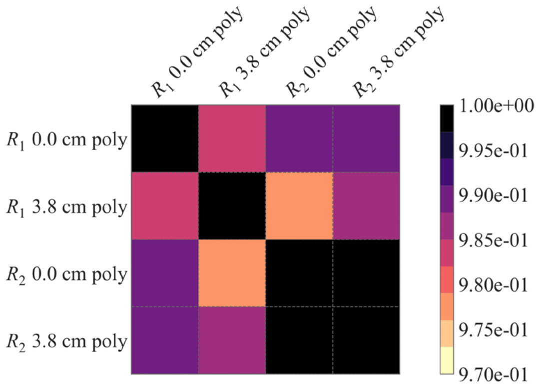

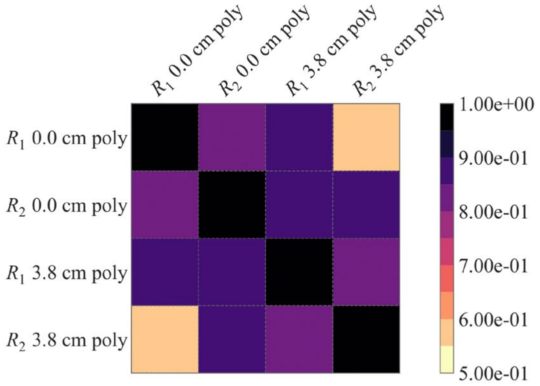

Correlations between the nominal (top-right) and adjusted (bottom-right) simulated responses due to the cross sections

Optimal adjustment to the Pu-239 $\bar{\nu}$

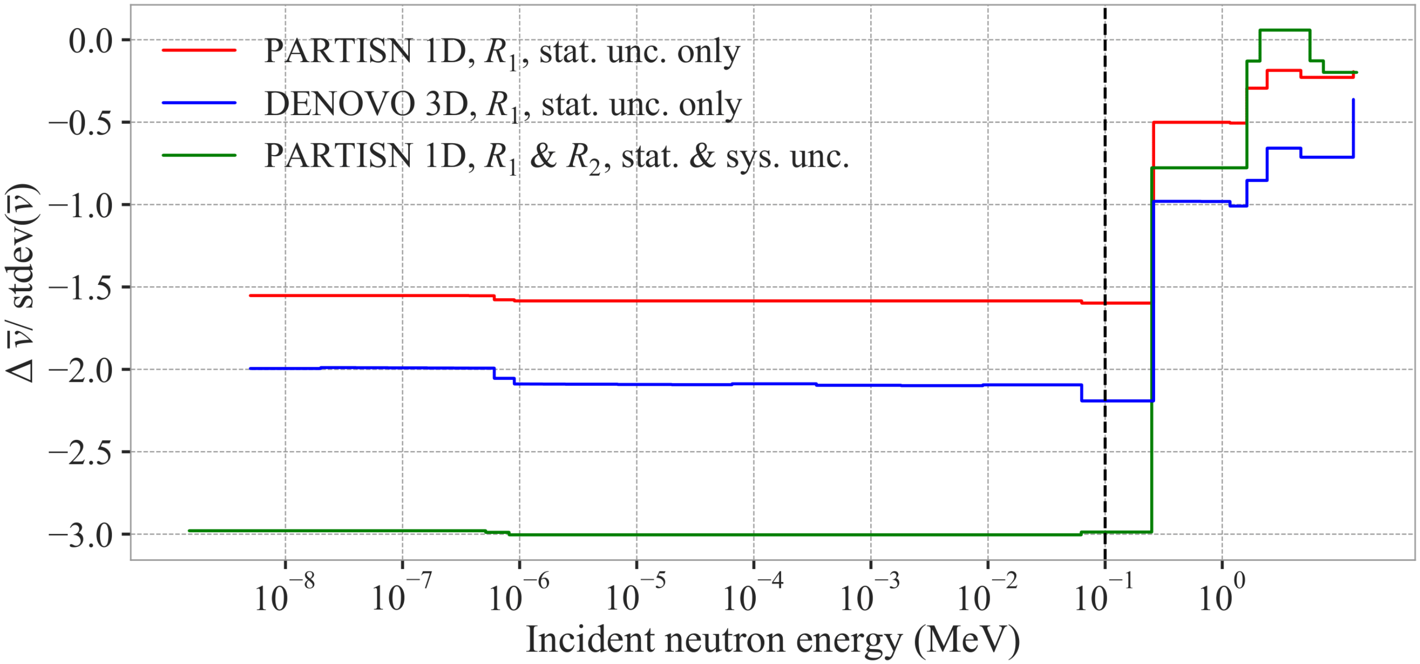

R_1 and R_2 comparison to experiment

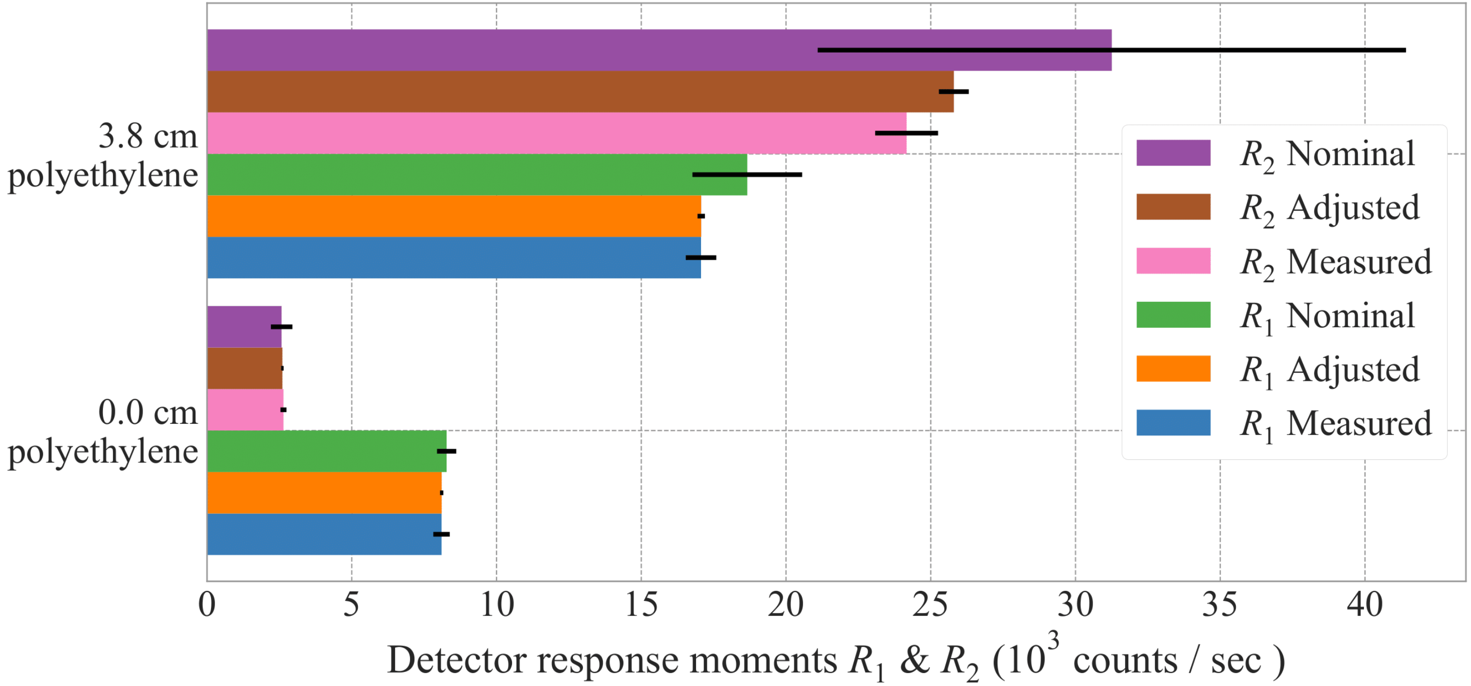

Summary and conclusions

- Calculated variance in the second moment detector response due to both random and systematic sources of uncertainty
- Applied an EKF to identify best-estimate cross sections and their covariances
- Demonstrated that NMC experiments were more accurately simulated with reduced uncertainty
- Adjustment to the cross sections is similar in trend to previous work but larger in magnitude due to inclusion of R_2 and systematic uncertainties

Outline

Dissertation research

- Introduction and motivation
- Model calibration process
- Model calibration applied to neutron multiplicity counting (NMC) measurements
- Summary and conclusions

Postdoctoral research

- Introduction and motivation
- Pulsed-sphere measurements
- SA applied to pulsed-sphere TOF spectra
- Summary and future work

Benefits to criticality safety

- Nuclear data adjustment accounting for random and systematic uncertainties resulted in improved neutron multiplicity counting simulations
- Combination of critical benchmarks and pulsed sphere measurements in nuclear data validation can provide tighter constraint on fission parameters

Identification of discrepant nuclear data with machine learning

- Deficiencies in nuclear data can have significant impact on many applications, including determining USLs for criticality safety
- Previous Machine Learning project had already identified discrepant nuclear data that most contributed to bias between measured and simulated critical benchmark responses (funded by NCSP-ASC [ATDM-PEM-V&V])
- LDRD-DR project, EUCLID, objective is "to design small-scale experiments that address needs and deficiencies in nuclear data"

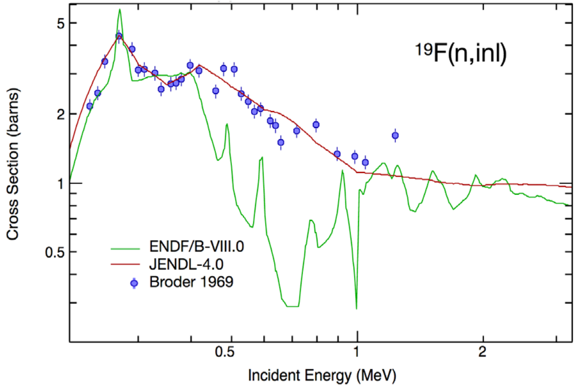

1. P. Grechanuk, M. E. Rising, and T. S. Palmer, "Using Machine Learning Methods to Predict Bias in Nuclear Criticality Safety," *J. Comput. Theor. Transp.*, 47:4-6, 552-565
2. D. Neudecker, O. Cabellos, A. R. Clark et al., "Enhancing Nuclear Data Validation Analysis by Using Machine Learning," Submitted Sept. 2019 to *Nucl Data Sheets*

Identification of discrepant nuclear data with machine learning

- Deficiencies in nuclear data can have significant impact on many applications, including determining USLs for criticality safety
- Previous Machine Learning project had already identified discrepant nuclear data that most contributed to bias between measured and simulated critical benchmark responses (funded by NCSP-ASC [ATDM-PEM-V&V])
- LDRD-DR project, EUCLID, objective is “to design small-scale experiments that address needs and deficiencies in nuclear data”

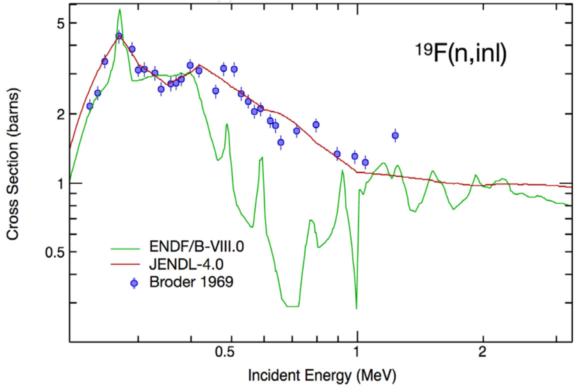

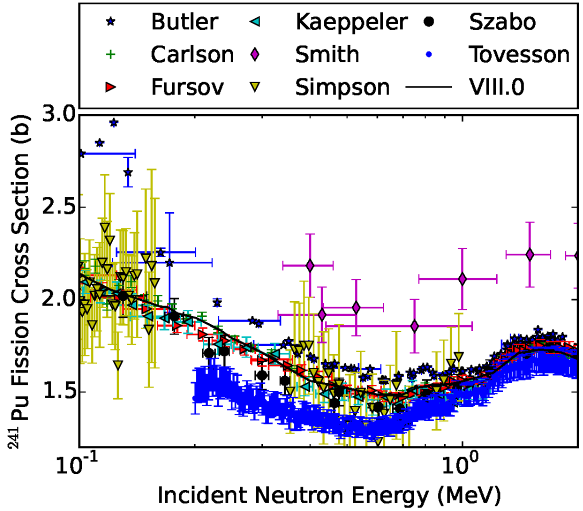

Optimal experiment design

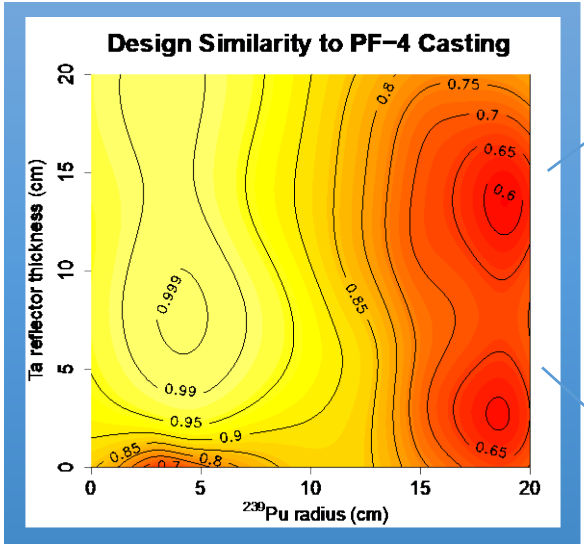

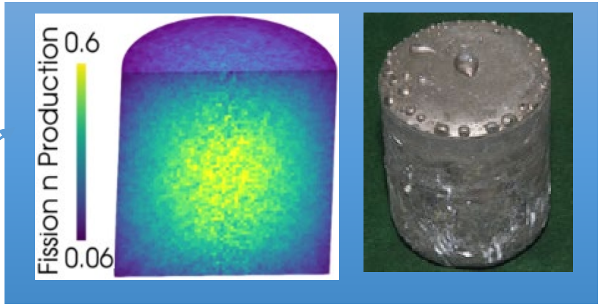

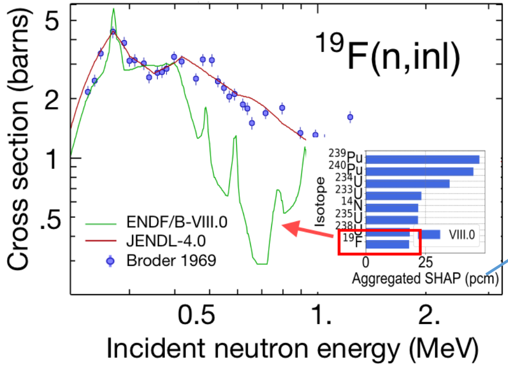

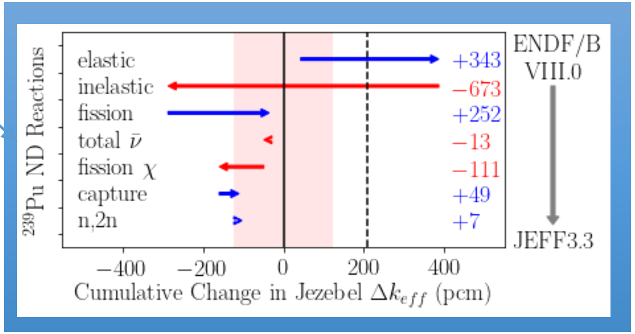

Justification for inclusion of diverse benchmarks

- Sometimes difficult to “disentangle” which nuclear data contributes to bias in critical benchmark
  - Single integral response from critical benchmark requires $\sim 10^6$ differential nuclear data points to simulate
  - Difficult to consider structural/moderator/reflector material separately from fissile core
  - Sensitive to a specific region of incident neutron energies
- One approach is to apply machine learning to a diverse set of measurements
  - Integral and differential observables (e.g. k_{eff} and TOF spectrum)
  - Composed of fissile and non-fissile materials
  - Sensitive to nuclear data in different energy regions
- Can improve nuclear data and benefit criticality safety

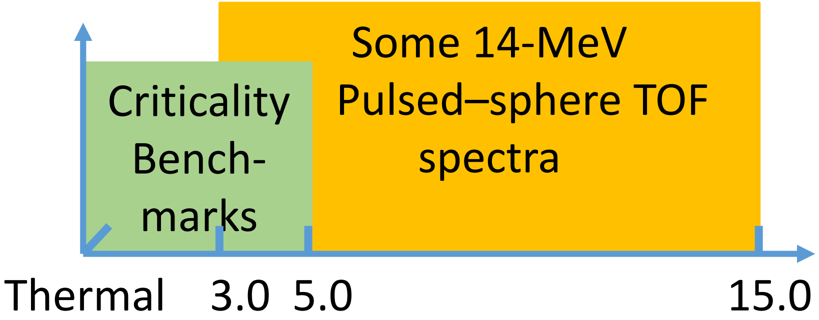

Nuclear data energy range to which simulations are sensitive (MeV)

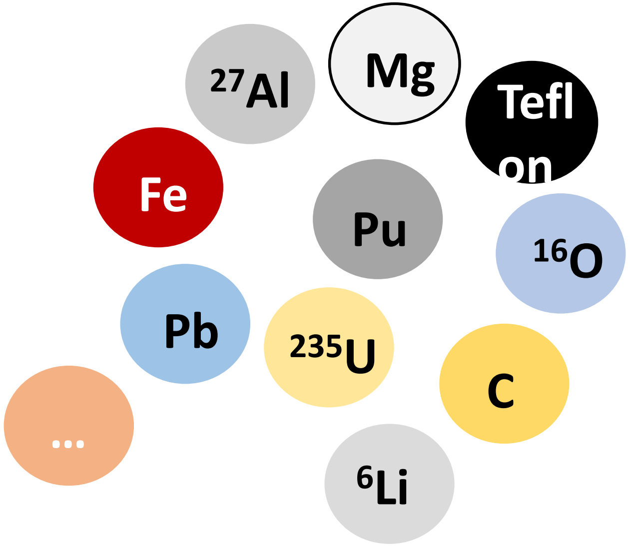

LLNL 14-MeV pulsed spheres

LLNL pulsed-sphere experimental setup

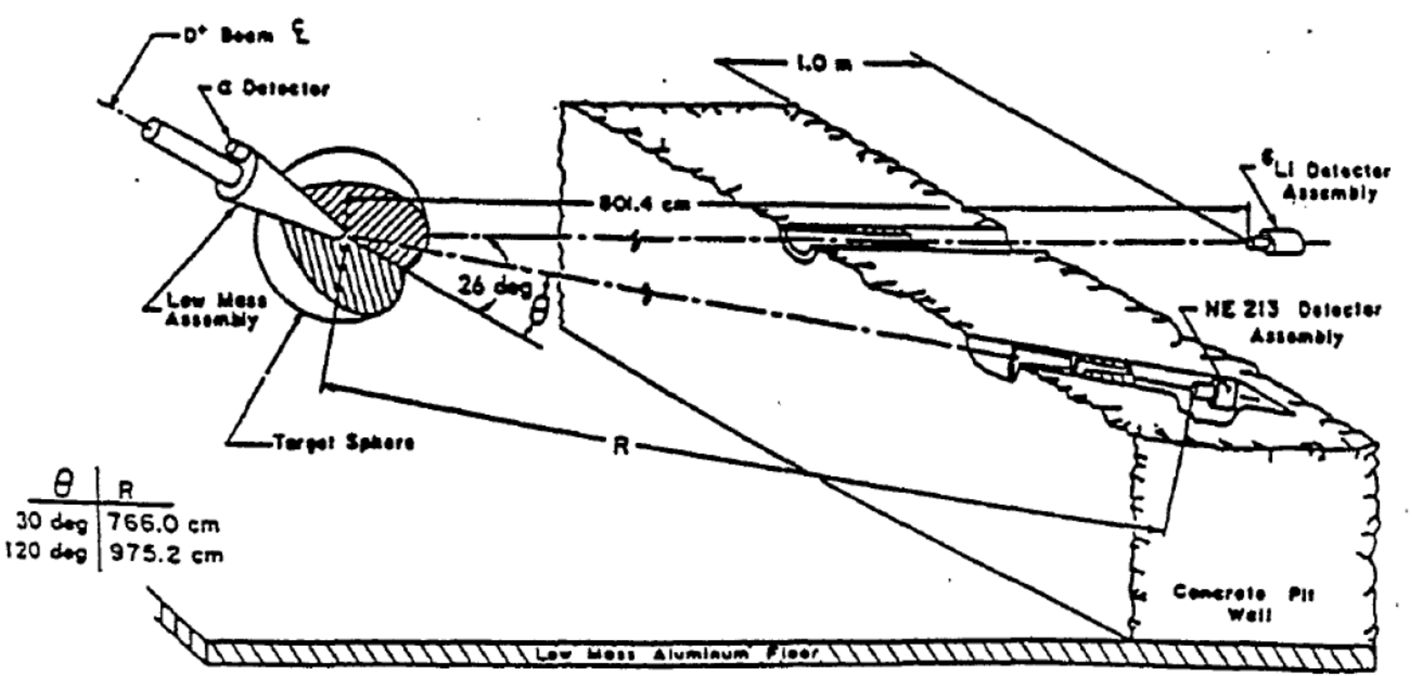

θ	R
30 deg	766.0 cm
120 deg	975.2 cm

1. Tanja Goričanec et al. “Analysis of the U-238 Livermore Pulsed Sphere Experiments Benchmark Evaluations,” International Nuclear Data Committee Report INDC(NDS)-0742 (2017)

Pulsed-sphere MCNP model

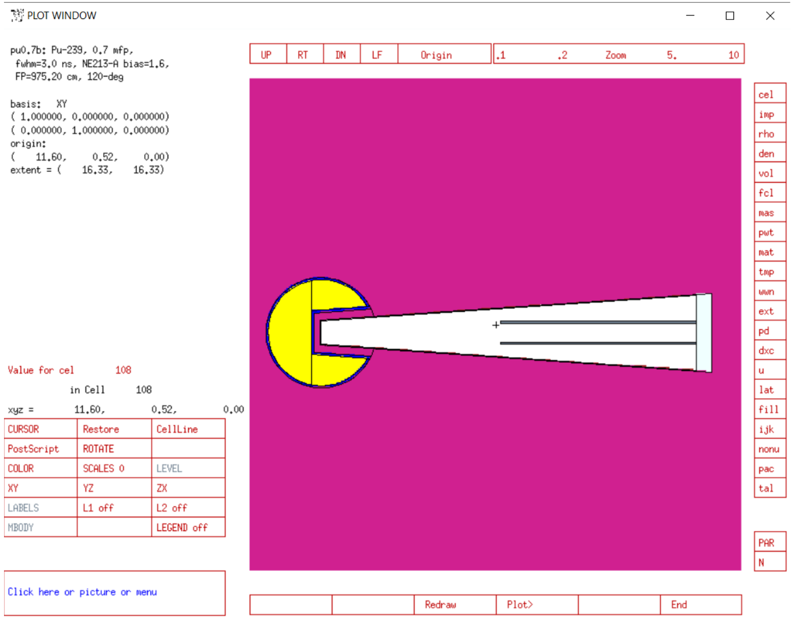

1. S.C. Frankle, “Possible Impact of Additional Collimators on the LLNL Pulsed Sphere Experiments (U)," LANL Report LA-UR-05-5877 (2005).
2. S.C. Frankle, “LLNL Pulsed Sphere Measurements and Detector Response Functions (U)," LANL Report LA-UR-05-5878 (2005).
3. S.C. Frankle, “README file for Running a LLNL Pulsed-Sphere Benchmark," LANL Report LA-UR-05-5879 (2005).

Pulsed-sphere MCNP model

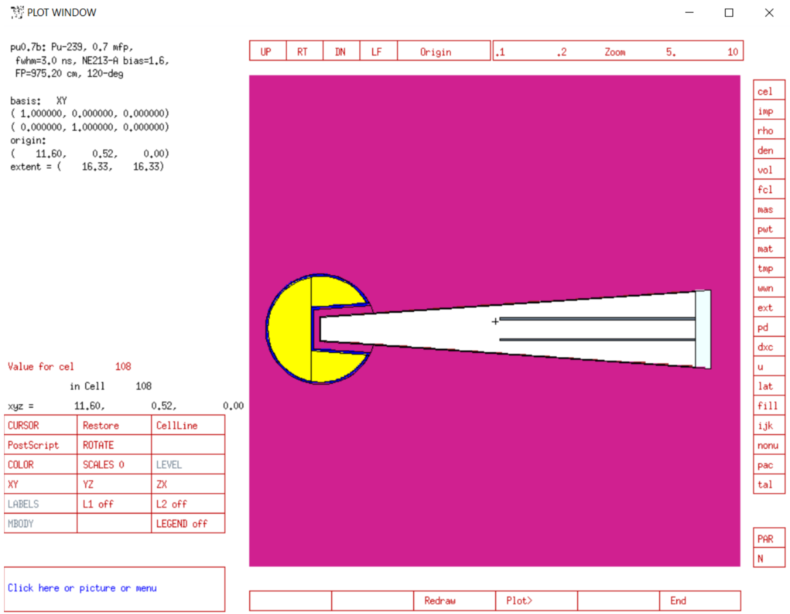

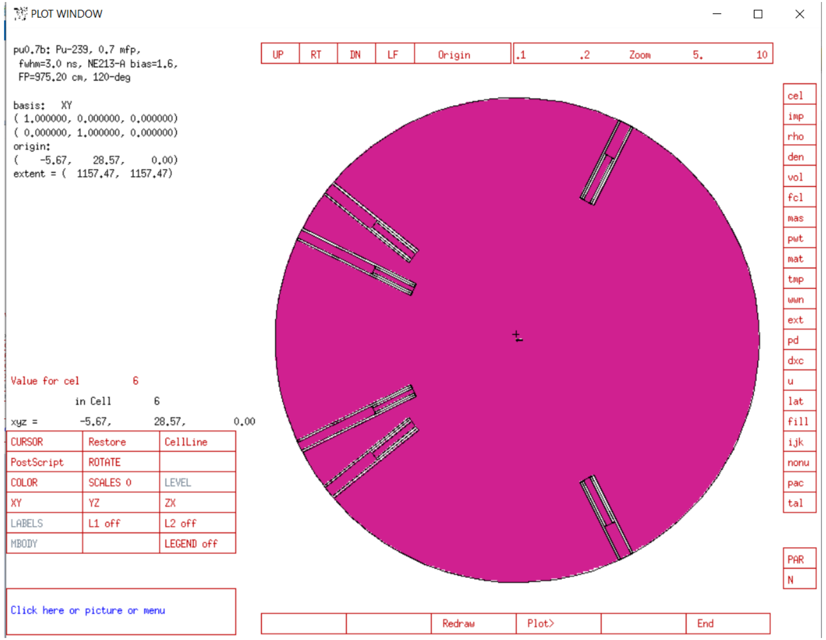

1. S.C. Frankle, “Possible Impact of Additional Collimators on the LLNL Pulsed Sphere Experiments (U)," LANL Report LA-UR-05-5877 (2005).
2. S.C. Frankle, “LLNL Pulsed Sphere Measurements and Detector Response Functions (U)," LANL Report LA-UR-05-5878 (2005).
3. S.C. Frankle, “README file for Running a LLNL Pulsed-Sphere Benchmark," LANL Report LA-UR-05-5879 (2005).

Simulated pulsed-sphere time-of-flight spectrum for plutonium pulsed sphere

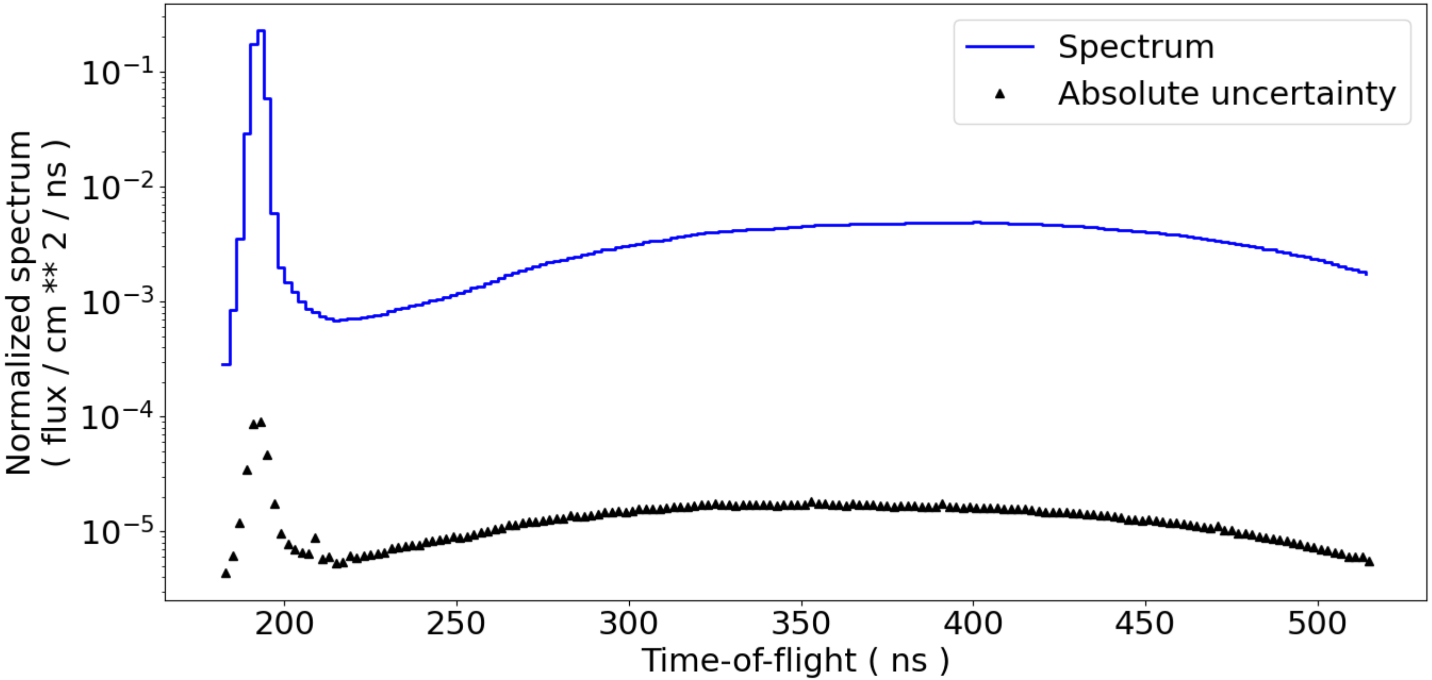

1. D. Neudecker, O. Cabellos, A. R. Clark et al, "Which nuclear data can be validated with LLNL pulsed-sphere experiments?," *manuscript submitted to ann. nucl. energy*, Jan. 6, 2021
2. W. Haeck, A. R. Clark, and M. Herman, “Calculating the impact of nuclear data changes with Crater,” *Trans. Am Nucl. Soc. Winter Meeting*, Online, Nov. 15-19, 2020

Estimating sensitivities with central-difference calculations

- Sensitivity of pulsed-sphere time-of-flight spectrum to group-wise nuclear data is defined as

$$S_{R_t,\alpha_g} = \frac{\alpha_{g,0}}{R_t|_{\alpha=\alpha_{g,0}}} \frac{\partial R_t}{\partial \alpha_g}\bigg|_{\alpha=\alpha_{g,0}}$$

  - R_t = Time-of-flight spectrum at time bin t
  - α_g = Nuclear data parameter at group g

- Sensitivity can be numerically estimated to second-order in perturbation size with central-differences

$$S_{R_t,\alpha_g} = \frac{\alpha_{g,0}}{R_t|_{\alpha=\alpha_{g,0}}} \frac{R_t|_{\alpha=\alpha_{g,0}+\Delta\alpha_g} - R_t|_{\alpha=\alpha_{g,0}-\Delta\alpha_g}}{2\Delta\alpha_g} + \mathcal{O}(\Delta\alpha^2)$$

Sensitivity analysis procedure

1. Obtain ENDF files from nndc.bnl.gov
2. Perturb nuclear data with one of two codes
   - FRENDY[1,3]
     - Process ENDF file into ACE format with NJOY
     - FRENDY directly perturbs ACE file
     - Operates on MF1,3
   - SANDY[2,3]
     - Process ENDF file into PENDF format with NJOY
     - SANDY perturbs either ENDF or PENDF file
     - Process ENDF and PENDF files in ACE format with NJOY
     - Operates on MF3,4
3. Generate MCNP input decks with Faust
4. Perform MCNP runs on HPC machine, Snow
5. Post-process MCTAL files with Faust to compute sensitivities[4]

1. K. Tada et al., “Development and Verification of a New Nuclear Data Processing System FRENDY,” *J.Nucl. Sci. Technol.*, **54**(7), pp. 806-817 (2017).
2. L. Fiorito, et al., “Nuclear data uncertainty propagation to integral responses using SANDY,” *Ann. Nucl. Energy*, Volume 101, 2017, Pages 359-366, ISSN 0306-4549.
3. O. Cabellos and L. Fiorito, “Examples of Monte Carlo Techniques applied for Nuclear Data Uncertainty Propagation,” *EPJ Web Conf.*, 211 (2019) 07008
4. W. Haeck, A. R. Clark, and M. Herman, “Calculating the impact of nuclear data changes with Crater,” *Trans. Am Nucl. Soc. Winter Meeting*, Online, Nov. 15-19, 2020

Pulsed Sphere TOF spectra enable studying fission-source term observables and angular distributions differently than criticality.

Critical benchmark

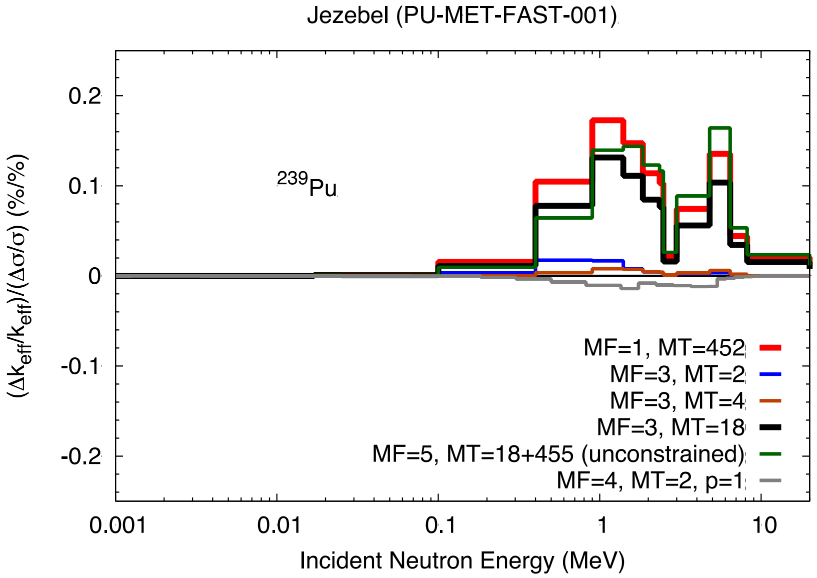

14-MeV LLNL pulsed sphere

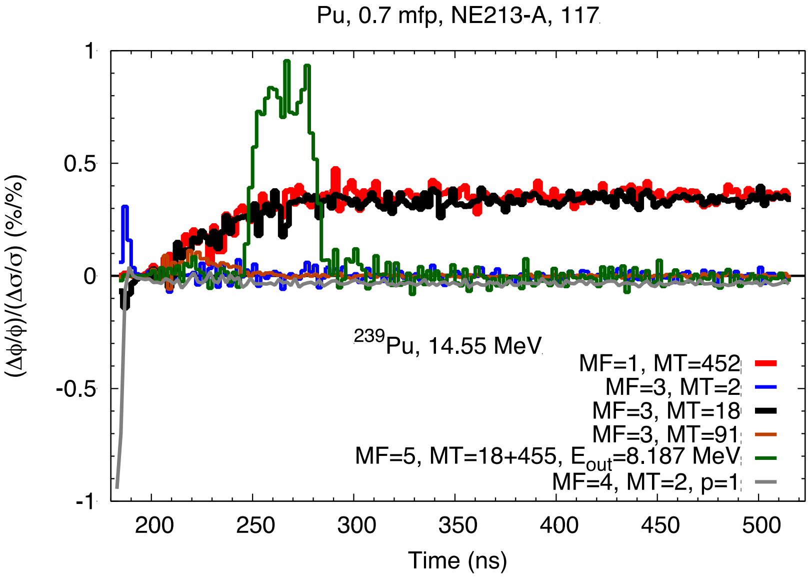

1. D. Neudecker, O. Cabellos, A. R. Clark et al, "Which nuclear data can be validated with LLNL pulsed-sphere experiments?," *manuscript submitted to ann. nucl. energy*, Jan. 6, 2021

Summary

- Difficult to disentangle which nuclear data contribute to bias between measured and simulated experiments
- Inclusion of diverse benchmarks (e.g. critical and pulsed spheres) can inform nuclear data evaluation for a greater number of nuclides and energy regions to benefit criticality safety
  - 2-MeV LLNL pulsed sphere measurements
  - Experiment campaigns at NCERC
- Developed Python tool, Pulsed Sphere Sensitivity Analysis toolkit (PSSAtk)
- EUCLID using PSSAtk to design small-scale experiments that address needs/deficiencies in nuclear data

Future work

- Finish pulsed-sphere sensitivity analysis and implement parts of it into Faust
- Develop tools in Faust for covariance processing and verification
  - Check whether covariances are physically meaningful
  - Make covariances accessible for end users
- Inform adjustment of nuclear data with pulsed-sphere sensitivity and uncertainty analysis
- Demonstrate additional constraint on fission parameters improves nuclear data adjustment and benefits criticality safety

Covariance-processing tools to benefit neutron-diagnosed subcritical experiments

- ENDF/B-VII.1 Pu-239 nu-bar reduced by ~1% to improved NMC simulations of the BeRP ball reflected by polyethylene
- ENDF/B-VII.1 U-235 inelastic scatter cross section reduced by ~20% to improve NDSE simulations of the Rocky Flats HEU shells reflected by polyethylene
- Expert knowledge identified these cross sections as high-impact to each problem
- ENDF/B-VII.1 release notes indicated that these cross sections had room in which to be adjusted
- Availability of covariance-processing tools could simplify identification and adjustment of problematic nuclear data

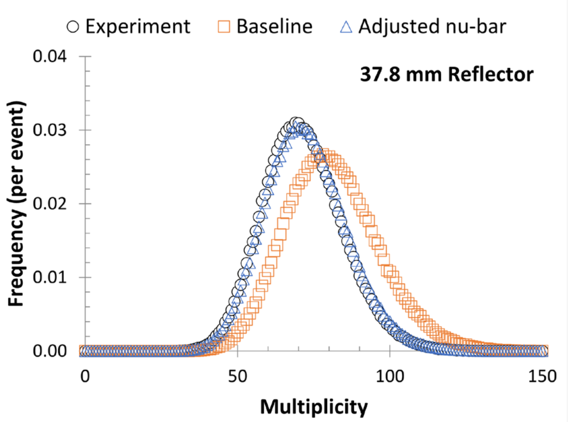

Simulated NMC distribution before and after Pu-239 $\overline{\nu}$ adjustment

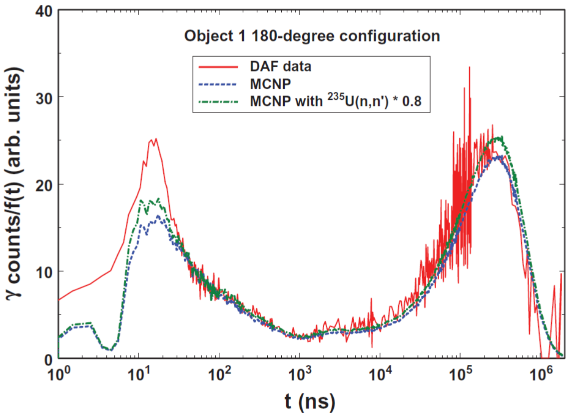

Simulated gamma coincidence data before and after U-235 (n, n') adjustment

Contributions to the literature

- D. Neudecker, O. Cabellos, **A. R. Clark** et. al, “Which nuclear data can be validated with LLNL pulsed-sphere experiments?,” Submitted to *Ann Nucl Energy*, Jan. 8, 2021
- J. Mattingly, **A. R. Clark**, and J. A. Favorite, “Application of Stochastic Neutron Transport Theory to Nuclear Data Evaluation using Subcritical Neutron Multiplicity Counting Experiments,” accepted in Aug. 2020 for M&C2021, Raleigh, NC, Apr. 11-15, 2021
- W. Haeck, **A. R. Clark**, and M. Herman, “Calculating the impact of nuclear data changes with Crater,” *Trans. Am Nucl. Soc. Winter Meeting*, Online, Nov. 15-19, 2020.
- **A. R. Clark, J. Mattingly, and J. A. Favorite, “Application of neutron multiplicity counting experiments to optimal cross section adjustments,” *submitted to Nucl. Sci. Eng.*, Sept. 2019**
- **A. R. Clark** et al., “Sensitivity analysis and uncertainty quantification of the Feynman Y and Sm_2,” *Trans. Am Nucl. Soc. Winter Meeting,* Orlando, Fl, Nov. 11-15, 2018
- **A. R. Clark** and J. Mattingly, "Data assimilation of nuclear cross sections applied to neutron multiplicity counting experiments", *Trans. Am Nucl. Soc. Annual Meeting*, Philadelphia, PA, Jun. 17-21, 2018, **Invited paper**

Supplemental content

Jezebel and BeRP ball assembly comparison

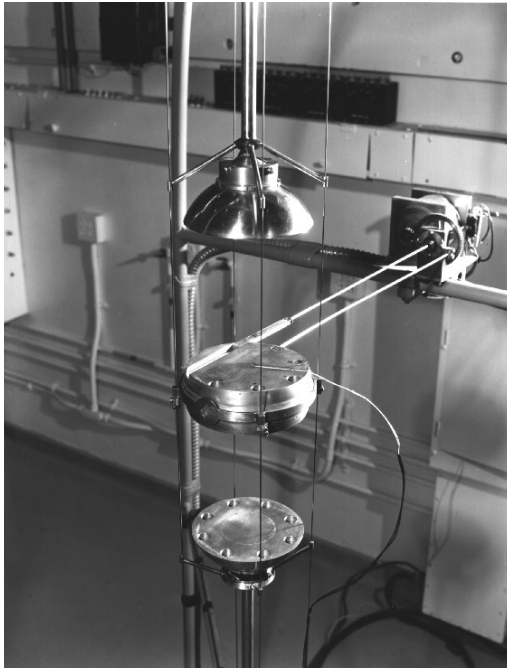

Jezebel is a fast, bare, critical assembly

The BeRP ball is a fast, polyethylene-reflected subcritical assembly

NMC distribution vs detector response moments

- NMC distribution $f(n)$
  - $\overline{n^q} = \frac{1}{N}\sum_{n=0}^{N} n^q f(n)$
  - $\mu_q = \frac{1}{N}\sum_{n=0}^{N}(n - \overline{n})^q f(n)$
  - $\overline{x}_{q,r} = \frac{1}{q!\,N}\sum_{n=q-1}^{N} n(n-1)\ldots(n-q+1)\, f(n)$
  - $\overline{x}_{1,r}$, $\overline{x}_{2,r}$, and $\overline{x}_{3,r}$ are called singles, doubles, and triples
- Only moments for $f(n)$ accumulated with large coincidence gate T are considered
- First-moment detector response $R_1 = \frac{\overline{n}}{T}$
- Second-moment detector response $R_2 = \frac{\mu_2 - \overline{n}}{T}$

Data assimilation applied to gross neutron counting

- Energy-dependent cross section adjustment via 3D DENOVO simulations of gross neutron counting of the BeRP ball
- Cross sections adjusted using Cacuci's data assimilation process
- Adjustment of Pu-239 $\overline{\nu}$ is between 1 and 2 standard deviations

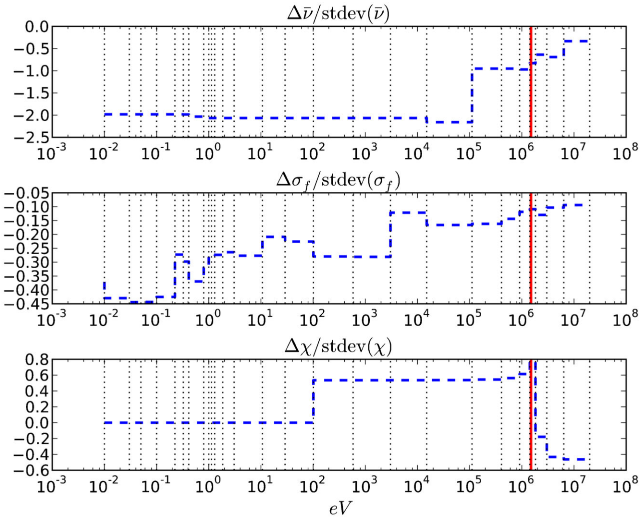

Adjustment to the Pu-239 $\overline{\nu}$ (top), σ_f (middle), and χ (bottom) in multiples of their respective standard deviations

Sensitivity of second-moment detector response

$$\frac{\partial R_2}{\partial \alpha} = \left\langle \psi_2^*, \frac{\partial Q}{\partial \alpha} - \frac{\partial L}{\partial \alpha}\,\psi \right\rangle + 2\left\langle \Phi, \frac{\partial Q_1^*}{\partial \alpha} - \frac{\partial L^*}{\partial \alpha}\psi_1^* \right\rangle + \left\langle \frac{\partial Q_2^*}{\partial \beta}, \psi \right\rangle + \left\langle \frac{\partial Q_{2,sf}^*}{\partial \beta}, S \right\rangle + \left\langle Q_{2,sf}^*, \frac{\partial S}{\partial \alpha} \right\rangle$$

$$\beta = \left\{ \overline{\nu(\nu-1)}, \overline{\nu(\nu-1)}_{sf} \sigma_f, \chi, \chi_{sf} \right\}$$

$$L\Phi = \left\{ I_1 \frac{\chi}{4\pi} \int d\Omega' \int dE' \overline{\nu(\nu-1)} \Sigma_f \psi \right\} + \left\{ I_{1,sf} \frac{\chi_{sf}}{4\pi} \int d\Omega' \int dE' \overline{\nu(\nu-1)}_{sf} S \right\}$$

- Φ is flux of fission neutrons that contribute to the second-moment detector response
- Second-moment detector response sensitivity calculable using standard transport solvers
- Can compute sensitivities for R_3 and higher-order moments in a similar way

Definition of sensitivity vector and total

- Element of $G \times 1$ relative sensitivity vector:

$$S_{R_q,\alpha_{g'}} = \frac{\alpha_{g'}}{R_q}\frac{\partial R_q}{\partial \alpha_{g'}}$$

- Scalar relative sensitivity total:

$$S_{R_q,\alpha} = \sum_{g'} S_{R_q,\alpha_{g'}}$$

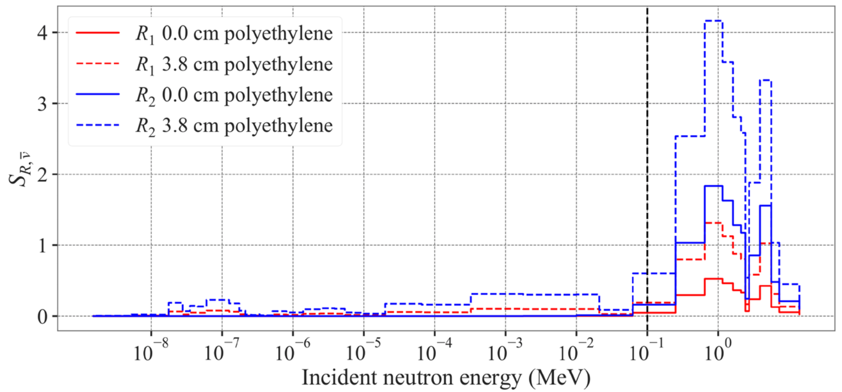

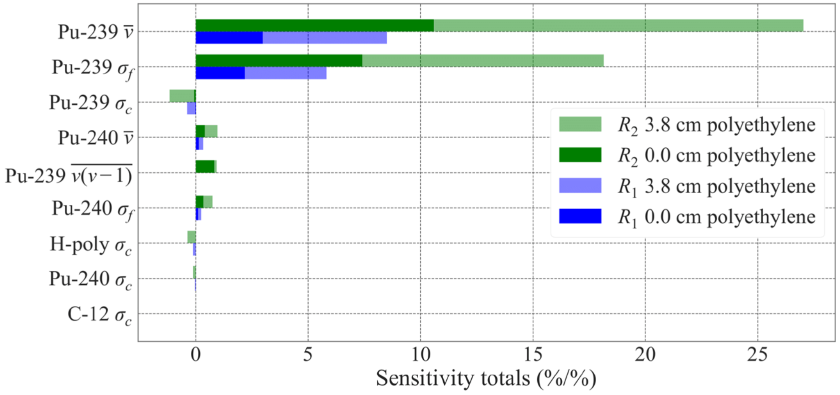

Sensitivity to fission cross section

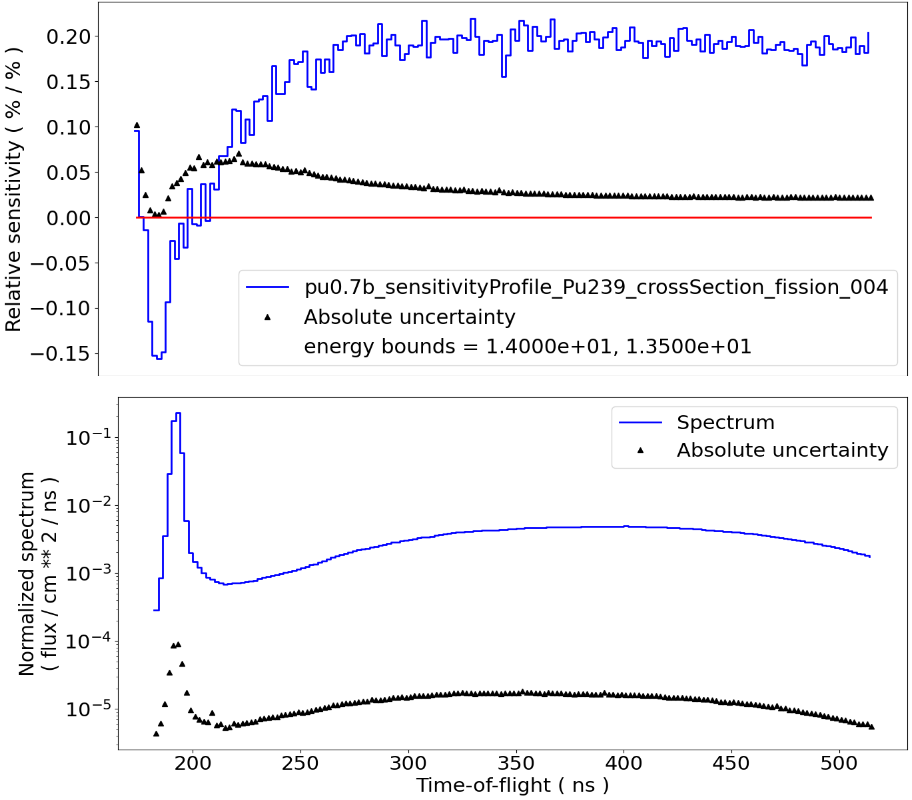

Sensitivity to fission cross section

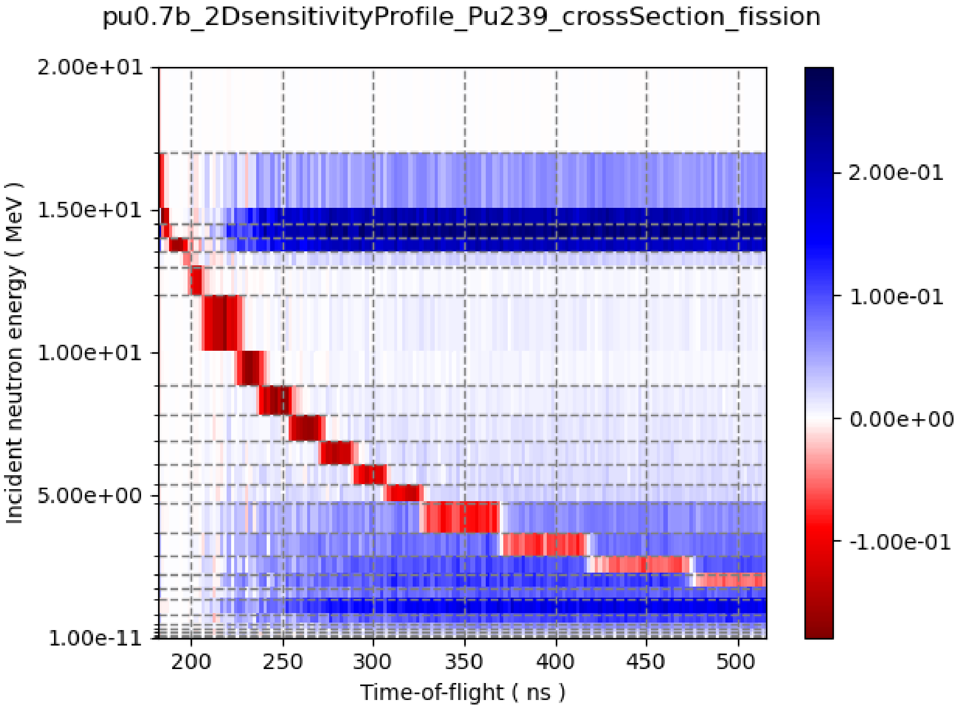

1. W. Haeck, A. R. Clark, and M. W. Herman, "Calculating the impact of nuclear data changes with Crater," Submitted for *Am. Nucl. Soc.* Radiation Protection and Shielding division meeting, Sept. 13-17, 2020